2002

Mass-Loss And Magnetospheres: X-Rays From Hot Stars And Young Stellar Objects

M. Gagné

David H. Cohen
Swarthmore College, dcohen1@swarthmore.edu

S. P. Owocki

See next page for additional authors

X-rays at Sharp Focus: Chandra Science Symposium
*ASP Conference Series, Vol. **VOLUME**, 2002*
eds. S. Vrtilek, E. M. Schlegel, L. Kuhi

Mass-Loss and Magnetospheres: X-rays from Hot Stars and Young Stellar Objects

Marc Gagné

Geology and Astronomy, West Chester University, West Chester, PA 19383

David Cohen

Physics and Astronomy, Swarthmore College, Swarthmore, PA 19081

Stanley Owocki and Asif Ud-Doula

Bartol Research Institute, University of Delaware, Newark, DE 19716

Abstract. High-resolution X-ray spectra of high-mass stars and low-mass T-Tauri stars obtained during the first year of the *Chandra* mission are providing important clues about the mechanisms which produce X-rays on very young stars. For ζ Pup (O4 If) and ζ Ori (O9.5 I), the broad, blue-shifted line profiles, line ratios, and derived temperature distribution suggest that the X-rays are produced throughout the wind via instability-driven wind shocks. For some less luminous OB stars, like θ^1 Ori C (O7 V) and τ Sco (B0 V), the line profiles are symmetric and narrower. The presence of time-variable emission and very high-temperature lines in θ^1 Ori C and τ Sco suggest that magnetically confined wind shocks may be at work. The grating spectrum of the classical T-Tauri star TW Hya is remarkable because the forbidden-line emission of He-like Ne IX and O VII is very weak, implying that the X-ray emitting region is very dense, $n_{\rm e} \approx 6 \times 10^{12}$ cm^{-3}, or that the X-rays are produced very close to the ultraviolet hotspot at the base of an accretion funnel. ACIS light curves and spectra of flares and low-mass and high-mass young stellar objects in Orion and ρ Ophiuchus further suggest that extreme magnetic activity is a general property of many very young stars.

1. Introduction

One of the early surprises from the *Einstein* mission was the detection of strong X-ray emission from O stars (Harnden et al. 1979). While the wind-shock paradigm for X-ray emission from hot stars (Lucy and White 1980; Owocki, Castor, & Rybicki 1988; MacFarlane & Cassinelli 1989; Hillier et al. 1993; Feldmeier et al. 1995; Cohen et al. 1996; Owocki & Cohen 1999) has gained acceptance over the past two decades, there is increasing evidence that not all early-type stars have X-ray properties that can be explained by instability-generated wind shocks alone. This evidence includes very hot plasma on the

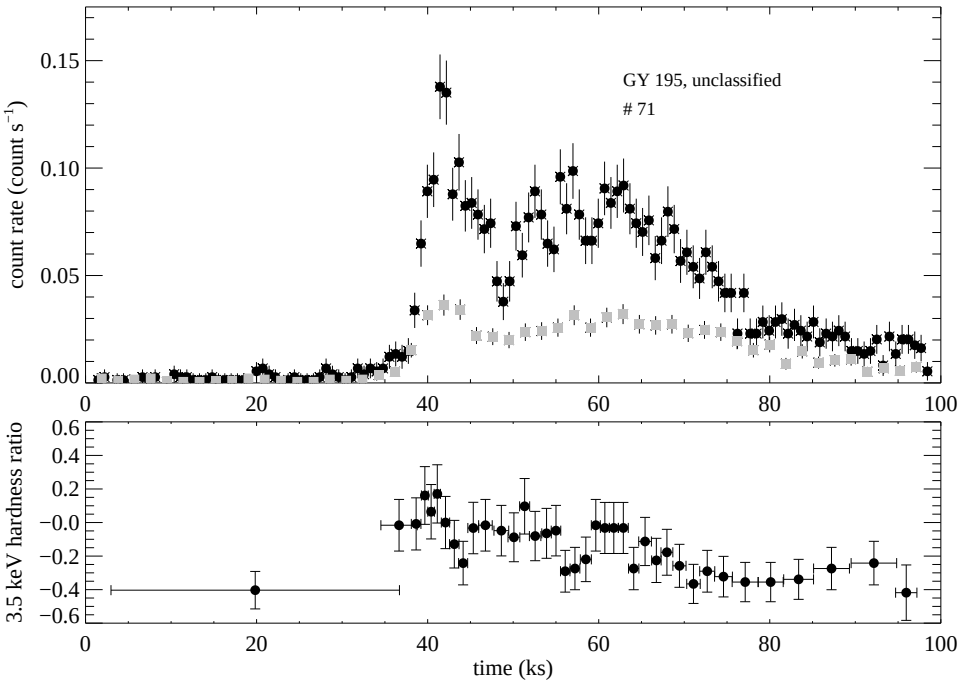

Figure 1. Hard-band (2.5-8.0 keV: black circles) and soft-band (0.5-2.5 keV gray squares) light curves of a flare on the T Tauri star (GY 195) in the ρ Oph A cloud. The ACIS flare spectrum can be fit with a single-temperature 4.7 ± 0.4 keV, low-Fe abundance ($Z = 0.25$) VMEKAL plasma with $N_{\rm H} = 3.9 \pm 0.1 \times 10^{22}$ cm^{-2}. The hard-band emission rises quickly at the onset of the flare and again during subsequent reheating events seen in the hardness ratio time-series (lower panel).

young B0 V star τ Sco (Cohen, Cassinelli, & Waldron 1997), overall levels of X-ray emission that approach or even exceed reasonable estimates of the wind emission measure in early- and mid-B stars (Cohen, Cassinelli, & MacFarlane 1997), and strong 15.4-day periodic X-ray emission on the central O star of the Orion Nebula, θ^1 Ori C (Gagné et al. 1997).

The lack of outer convection zones in hot stars, and the lack of any correlation between X-ray activity and rotation (Pallavicini et al. 1981) has been taken to mean that the X-rays from early-type stars are not produced by magnetic activity associated with a solar-type dynamo. However, it has been suggested that large-scale magnetic fields, in conjunction with radiation-driven winds, could play a role in the X-ray production on some of these early-type stars (e.g., Babel & Montmerle 1997a). The strong and hard X-ray emission from θ^1 Ori C, τ Sco, as well as several other young hot stars (Corocoran et al. 1994; Yamauchi et al. et al. 1996; Schulz et al. 2000), suggest that some type of magnetic confinement, possibly associated with youth, may lead to the efficient production of hard X-rays on some hot stars. If the magnetic fields on hot stars survive

the star-formation process, the transfer of angular momentum via a magnetized wind would lead to significant spin down.

The discovery of strong variable X-ray emission from classical T-Tauri stars (CTTS) in Taurus-Auriga with *Einstein* (Gahm et al. 1980) was less surprising because TTSs were known to be relatively fast rotators, strong Hα sources, and to undergo strong white-light flares. Since then, large-amplitude, long-duration flares have been observed many times with *Einstein*, *ROSAT*, *ASCA*, and *Chandra*. The temperature of the flaring plasma rises from a quiescent value of 6–20 MK to a peak value of 50–100 MK in minutes to hours and decays on time scales of many hours. The central question is whether TTSs have very active solar-type coronae driven by a magnetic dynamo or whether flares are produced in some kind of a magnetosphere coupled to a disk.

The X-ray flare spectra and light curves have been modeled in two ways: as a single heating event in a quasi-statically cooling magnetic loop and as a series of heating events in a coronal active region. E.g., a giant *ASCA* flare on the weak-line T-Tauri star (WTTS) V 773 Tau showed a peak temperature of 100 MK and a decay time of 2.3 hours (Tsuboi et al. 1998). A quasi-static cooling loop approximation implies moderate electron densities like those observed in solar flares and very large loop lengths, $l \gtrsim R_\star$. Favata, Micela, & Reale (2001) have modeled the same flare data hydrodynamically to show that such flares may be produced in much smaller loops. In this model, long-duration flares are a manifestation of continuous reheating events rather than a single flare in a large, low-density loop.

ASCA flares on three young stellar objects (YSOs) in ρ Ophiuchus, YLW 15, WL 6, and Elias 29, showed evidence of rotational modulation, quasi-periodic flaring, and significant spectral time variability (Tsuboi et al. 2000). Montmerle et al. (2000) present a magnetosphere/disk interaction model to explain the quasi-periodic flares on the Class I YSO YLW 15. Again, Favata, et al. (2001) show that such flares may reflect reheating events in high-latitude active regions.

The recent discovery of X-ray emission from deeply embedded submillimeter/radio dust condensations in the Orion molecular cloud (Tsuboi et al. 2001) indicates that magnetic heating begins at the earliest stages of star formation. It remains to be seen whether the large-scale magnetic fields which are believed to regulate accretion, mass-loss, and bipolar outflows are related to the reconnection events which lead to flares and X-ray activity.

Disk-photosphere coupling via a magnetic field was first suggested by Königl (1991) (inspired by the model of Ghosh & Lamb 1979) to explain the slow rotation of CTTSs. A recent study of low-mass 1-30 Myr stars in the Orion Nebula Cluster and NGC 2264 (Rebull et al. 2001) found that PMS stars evolve with nearly constant angular velocity as they contract down their convective tracks. This means that the mechanism which regulates the spin of a CTTS may still be at work on WTTSs long after a dusty disk has been dissipated. If magnetic coupling still operates long into the WTTS phase, then a gas (plasma) disk must exist within a few stellar radii of the photosphere.

In this paper we will discuss recent *Chandra* results which address magnetic activity on young high-mass and low-mass stars. §2 summarizes results based on *ASCA* and *Chandra* light curves and CCD spectra of YSO flares in ρ Ophiuchus. In §3 we describe the X-ray grating spectrum of the CTTS TW Hya and use the

forbidden lines of Ne IX and O VII to suggest a location for the X-ray emitting plasma. In §4 we describe grating spectra of four hot stars that, in some cases, provide strong evidence for magnetic confinement. In §5 we present 2-D MHD simulations of magnetically confined wind shocks. Finally, we conclude that magnetic fields, disks, and mass-loss may play a central role in the production of X-rays on very young high-mass and low-mass stars.

2. Young Stellar Objects in ρ Ophiuchus

The ρ Ophiuchus A cloud was observed continuously for 96 ks with ACIS-I on 2000 May 15. An RGB image of the fiterered event data with red=soft (0.5-1.5 keV), green=medium (1.5-2.5 keV), and blue=hard (2.5-8 keV) shows 76 X-ray sources. Highly absorbed YSOs and background AGN seen through 25-75 mag of visual absorption appear as blue sources in this image. Twenty-two background AGN have been identified as faint sources with high 2-keV hardness ratios and low Kolmogorov-Smirnov variability statistics. By dividing the event data into 31 time bins and removing flickering background pixels, we have produced a color movie illustrating what Montmerle et al. (1983) described as an "X-ray Christmas Tree" in ρ Oph.

In Figure 1, we present ACIS medium- and hard-band light curves of the low-mass YSO GY 195 in ρ Oph A. The lower panel is the time-series of 3-keV hardness ratios for GY 195. This flare is interesting because of the deep dip in the hard-band ($3-8$ keV) light curve approximately 48 ks after the start of the observation. Initially, we interpreted this as evidence of self-eclipsing. However, the soft-band ($0.5-3$ keV) light curve shows a much smaller dip than expected. Since the emission-measure distribution at the peak of a flare is dominated by very hot plasma ($T > 50$ MK), those times of the when the hard emission rises sharply probably correspond to reheating events. We see a few small flare events before the major peak at 41 ks, a rapid decay, and a series of reheating events at approximately 52, 62, 83, and 93 ks. We have yet to perform a detailed spectral time-series analysis on these data, but our initial XSPEC analysis suggests a very hot, low-abundance coronal plasma, and high column density consistent with other embedded T Tauri stars in ρ Oph.

The ρ Ophiuchus cloud contains two optically visible stars: the young, magnetic B3 star S1 Oph and the WTTS DoAr 21. During the *Chandra* observation, DoAr 21 was in the decay phase of a very large flare. Although no major flares were seen on S1, the light curve exhibits low-amplitude, long-term and short-term variability. The ACIS spectrum of this high-mass YSO is reminiscent of low-mass YSOs: $N_{\rm H} = 4.1 \pm 0.5 \times 10^{22}$ cm^{-2} and $kT = 3.1 \pm 0.5$ keV. Simultaneous VLA observations at 2 and 6 cm show variable, non-thermal radio emission, confirming its magnetic origin, first reported by André et al. (1993). S1's radio and X-ray properties make it a good candidate for magnetically confined wind shocks (see §5).

3. The Classical T Tauri Star TW Hya

With the launch of *Chandra* and *Newton*-XMM, high-resolution grating spectroscopy has become an important new tool for studying X-ray activity on young

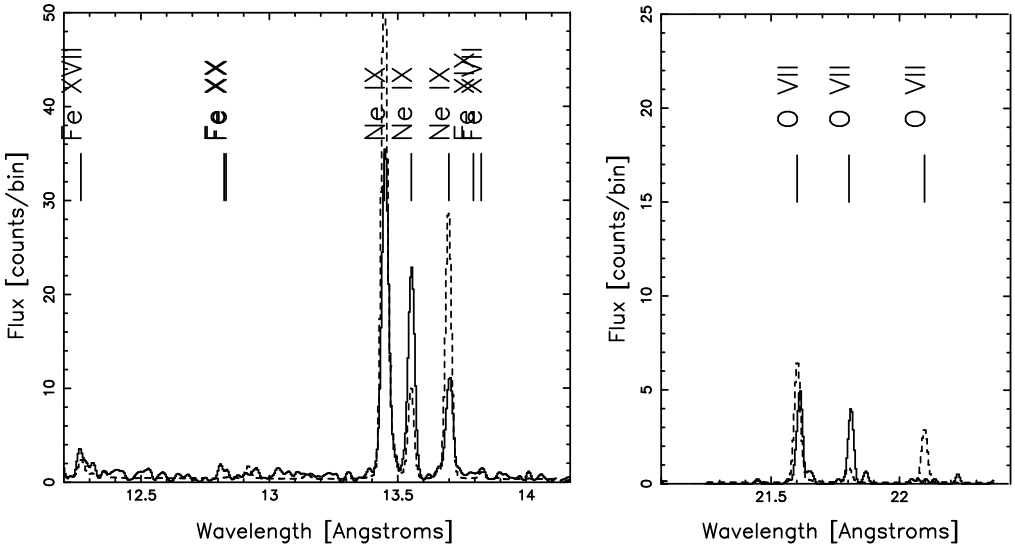

Figure 2. The MEG spectrum (solid lines) of TW Hya around the rif Ne IX and O VII triplets (Kastner et al. 2001). The observed spectrum is overlaid with a variable-abundance, differential emission-measure model (dashed curve) that best-fits temperature-sensitive lines. Note the discrepant intercombination and forbidden lines.

stars. The He-like resonance (r), intercombination (i), and forbidden (f) lines of coronal sources like AB Dor (dotted line in Fig. 2) are useful density diagnostics because the collisional excitation rate from the metastable $^1S_1$ state depends on density (see Figure 1 of Gabriel & Jordan 1969). The critical density is reached when the collisional excitation rate equals the forbidden $^3S_1 \rightarrow {}^1S_0$ photodecay rate. For AB Dor, the forbidden-line emission is strong; the S, Si, Mg, and Ne f/i ratios are close to their low-density limits. The O VII f/i ratio yields $\log n_e = 10.68 \pm 0.33$ cm^{-3}.

For TW HYa, a classical T Tauri star, the f lines of Ne IX (seen in Fig. 1) and O VII are remarkably suppressed. Kastner et al. (2001) measure $f/i = 0.44 \pm 0.13$ for Ne IX indicating $\log n_e = 12.75 \pm 0.15$ cm^{-3}. This is the highest coronal density measured so far using f/i ratios, exceeding that of AB Dor by two orders of magnitude, possibly signaling a fundamental difference between coronal stars and T Tauri stars. Kastner et al. go further, suggesting that the bulk of the X-ray emission on TW Hya is generated at the base of the accretion funnel which couples the accretion disk to the stellar photosphere.

We point out, however, that ultraviolet emission can depopulate the metastable $^3S_1$ state via photoexcitation to the $^3P_{210}$ state (see Kahn et al. 2001). The forbidden line is suppressed when the $^3S_1 \rightarrow {}^3P$ photoexcitation rate R_{PE} approaches the $^3S_1 \rightarrow {}^1S_0$ photodecay rate R_{RD}. For O VII and Ne IX photoexcitation occurs in the ultraviolet at 1616 and 1246Å. The photoexcitation rate for the metastable state of Ne IX is $R_{PE} = F_\nu \frac{\pi e^2}{mc} f$, where $f = 0.0949$ (Cann & Thakkar 1992). $R_{PE} = R_{RD} = 1.09 \times 10^4$ s^{-1} (Drake 1971) implies a critical flux $F_\nu = 4.33 \times 10^6$ s^{-1} cm^{-2} Hz^{-1}. TW Hya's flux at 1245.8 Å from the IUE

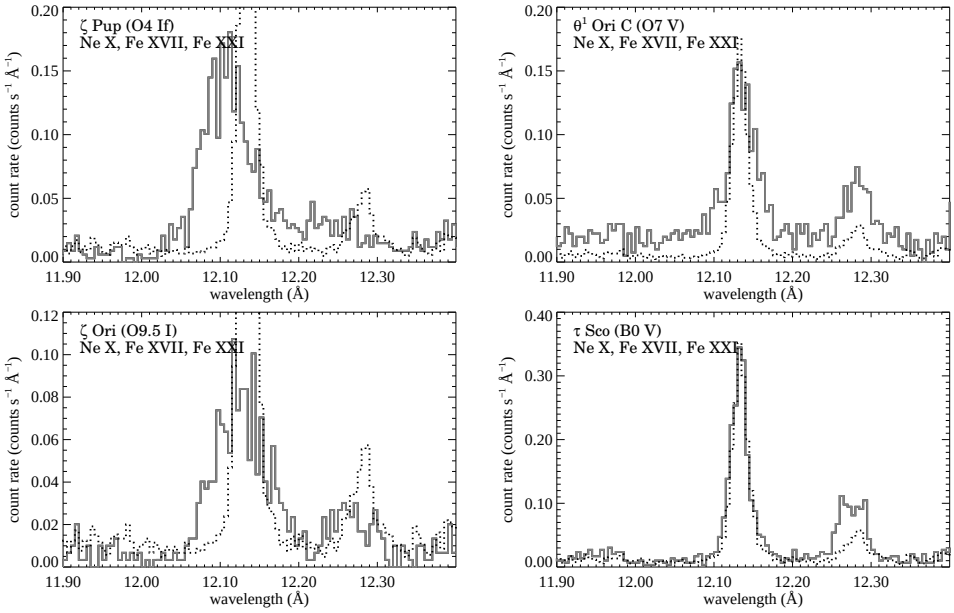

Figure 3. MEG spectra (solid gray lines) of ζ Pup (upper left panel) and θ^1 Ori C (lower panel). The MEG spectrum of AB Dor (K0 V) is shown (dashed line) for comparison. As expected for a luminous hot star with instability driven wind shocks, the Ne X resonance line of ζ Pup is blueshifted, broad, and asymmetric. The Ne X line of θ^1 Ori C (upper right panel) is symmetric about line center and its non-thermal, non-instrumental width is $v \approx 410$ km s^{-1}. Note the strong Fe XXI line. ζ Ori (lower left panel) shows a broad Ne X line. The τ Sco lines (lower right panel) are narrow, like those of the coronal source AB Dor (dashed line).

archive is $f_\lambda \approx 3.5 \times 10^{-14}$ ergs s^{-1} cm^{-2} Å^{-1}. We consider the simplest geometrical model: a star at a distance D (56.4 pc for TW Hya) with X-ray and UV sources separated by a distance d. In this case, $F_\nu = (D/d)^2 f_\nu$. Solving for the UV/X-ray separation at which $R_{\rm PE} = R_{\rm PD}$, we find $d \approx 2.5 \times 10^9$ cm, i.e., $d \approx 0.04 R_\odot$.

On TW Hya, the O VII forbidden line is strongly suppressed. Assuming $R_{\rm PD} = 1.04 \times 10^3$ s^{-1} and $f = 0.0742$ implies a critical incident flux $F_\nu = 5.28 \times 10^5$ s^{-1} cm^{-2} Hz^{-1}. TW Hya's IUE flux at 1616.5 Å is $f_\lambda \approx 3.0 \times 10^{-14}$ ergs s^{-1} cm^{-2} Å^{-1}, implying a critical UV/X-ray separation $d \approx 1.1 \times 10^{10}$ cm. Since the O VII f line is entirely suppressed, $d < 0.16 R_\odot$. Thus, the Ne IX and O VII f/i ratios may be suppressed via ultraviolet photoexcitation, provided the X-rays are produced close to the UV continuum source.

We note that T Tauri stars have strong UV emission lines (H I, N V, C IV, Si IV) produced by optically thin $5 \times 10^4 - 2 \times 10^5$ K plasma. The continuum emission (which depopulates the $^3S_1$ state) is not produced by an optically thin transition region. If this thick material is distributed over much of the photosphere, the UV continuum would be too diluted to suppress the O VII

and Ne IX forbidden lines. The forbidden lines are suppressed if the X-rays are emitted at the base of the accretion funnel directly above the optically thick UV hotspot.

An alternate hypothesis is that X-ray emitting magnetic loops are distributed throughout an active corona. In this case, the f/i ratios are unaffected by UV flux and $\log n_{\rm e} \approx 12.75$ cm^{-3}, the total particle density $n = 1.77 n_{\rm e}$, the mean temperature in the loop is at the peak of the emission-measure distribution $T \approx 3.0 \times 10^6$ K, and the total gas pressure in the loop is $P = nkT = 4.12 \times 10^3$ dynes cm^{-2}. The mean magnetic field strength required to confine such a loop is $B^2 \geq 8\pi nkT \Rightarrow B \geq 320$ G. Direct measurements of magnetic field strengths and filling factors on other T Tauri star indicate very strong 1–4 kG fields concentrated in cool spots covering a large fraction of the photosphere (Johns-Krull, Valenti, & Koresko 1999; Guenther et al. 1999). Even allowing for the geometric reduction in the magnetic intensity as loops expand into the corona, coronal loops on T Tauri stars can sufficiently confine high-density coronal plasma.

In conclusion, X-ray and far-UV spectra of T Tauri stars may provide a key test of accretion-powered X-ray activity. If the forbidden lines are suppressed by photoexcitation, Si XIII, Mg IX, Ne IX, and O VII f/i ratios will yield self-consistent estimates of the UV/X-ray source separation.

4. X-ray Grating Spectra of OB stars

The far-ultraviolet flux from OB stars is $10^5 - 10^6$ times brighter than on T Tauri stars like TW Hya. As a result, O VII and Ne IX f-line emission is essentially absent. The $^3S_1 \rightarrow {}^3P$ transitions of Mg XI and Si XIII at 1024.4 Å and 901.8 Å, respectively, are used to estimate the average distance bewteen the photosphere and the X-ray emitting region. Kahn et al. (2001) and Cassinelli et al. (2001) have shown for ζ Pup (O4 If) that the visible X-rays are emitted $1 - 5 R_\star$ from the photosphere where the overlying wind becomes optically thin at the wavelengths of Mg XI, Si XIII, and S XV. These results indicate that X-ray emitting regions are distributed throughout the wind as predicted by instability-driven wind shock theory. ζ Pup's X-ray line profiles provide further confirmation of this picture. In the upper left panel of Figure 3, the 12.1 Å Ne X line of ζ Pup is blueshifted, broad, and asymmetric because the optically thick wind absorbs most of the X-rays from receding shocked material on the far side of the star. The challenge for wind shock models is to produce strong enough shocks at the base of the wind to explain the Si XIII and S XV emission.

While high-resolution spectra of ζ Pup support the distributed wind-shock hypothesis, HETG spectra of three other hot stars are more difficult to explain. In Fig. 3, the Ne X line of θ^1 Ori C (O7 V) and τ Sco (B0 V) do not show obvious line asymmetries. In their analysis of the θ^1 Ori C spectrum, Schulz et al. (2000) find a range of line widths ($300 - 800$ km s^{-1}) and no systematic line shifts. Schulz et al. (2000) state that these results are consistent with instability-driven wind shocks. However, Owocki & Cohen (2001) have shown that the substantial amount of emission longward of line center is difficult to reconcile with the expected attenuation by the wind. Based on f/i ratios, Waldron & Cassinelli (2001) find that the hottest plasma around ζ Ori must lie less than

$1R_\star$ from the photosphere, concluding that wind shocks and some magnetic confinement of turbulent hot plasma may be required. The τ Sco lines are narrow and may not be produced in outflowing material many stellar radii from the photosphere.

The 10–12 Å spectra of ζ Pup, θ^1 Ori C, and τ Sco also exhibit striking differences. ζ Pup (see Figure 3 of Cassinelli et al. 2001 and Figure 5 of Kahn et al. 2001) shows broad, asymmetric, blue-shifted lines of Ne IX and Fe XVII, indicating little emission measure above 10 MK. The 10–12 Å MEG spectra of θ^1 Ori C and τ Sco in Figure 4 show very strong, narrow, symmetric Fe XXIII and Fe XXIV lines suggesting very hot ($T > 16$ MK), solar-abundance plasma (Schulz et al. 2000). To date, instability-driven wind shock models cannot produce such high-temperature shocks, especially not on OB stars like θ^1 Ori C and τ Sco with relatively low mass-loss rates and terminal wind speeds.

5. Magnetically Confined Wind Shocks

The leading theoretical picture for X-ray production in magnetized hot stars is the magnetically confined wind shock (MCWS) model proposed by Babel & Montmerle (1997a) and applied by the same authors to θ^1 Ori C (1997b). In this model, an ionized, radiation-driven wind is confined to flow along a magnetic dipole field and is thus channeled, at low latitudes, into the magnetic equatorial plane. In the magnetic equator, the streams from the two hemispheres collide and are confined by the dipole field, producing a standing shock and X-ray emission above and below a disk-like feature above the magnetic equator.

This model succeeds in producing relatively hard X-rays (due to the nearly head-on collision of two fast streams), high levels of emission (due to the confinement at relatively high densities of the shock-heated plasma), and rotational modulation of the X-rays, like that observed in θ^1 Ori C, if the dipole field is tilted with respect to the rotational axis. This oblique magnetic rotator model has been used to explain many of θ^1 Ori C's curious behaviors: periodic Hα and He II emission and periodic C IV and Si IV P-Cygni profiles (Stahl et al. 1993; Walborn & Nichols 1994; Stahl et al. 1996; Reiners et al. 2000). Based on circular spectro-polarimetric monitoring of its Balmer lines, Jean-François Donati and collaborators have recently measured a polar magnetic field strength $B \approx 1.1$ kG (2001, private communication) at phase 0.0. This implies that X-ray, Hα and He II emission is greatest when looking down on the magnetic pole (phase 0.0). Emission is weakest when looking at the magnetic equator (phase 0.5), presumably because hot plasma just above the magnetic equator is eclipsed by the photosphere. We note that Stahl et al. and Babel & Montmerle proposed the opposite magnetic geometry.

The model of Babel & Montmerle, which assumes a rigid magnetic geometry, has been extended to allow the magnetic field morphology to be modified by the wind flow in a self-consistent manner (Ud-Doula & Owocki 2001, in preparation). Assuming an initially dipolar field and spherical mass-loss, the 2-D MHD code simulates the time evolution of density, temperature, and velocity throughout the wind. A given set of field strength and wind parameters defines a confinement

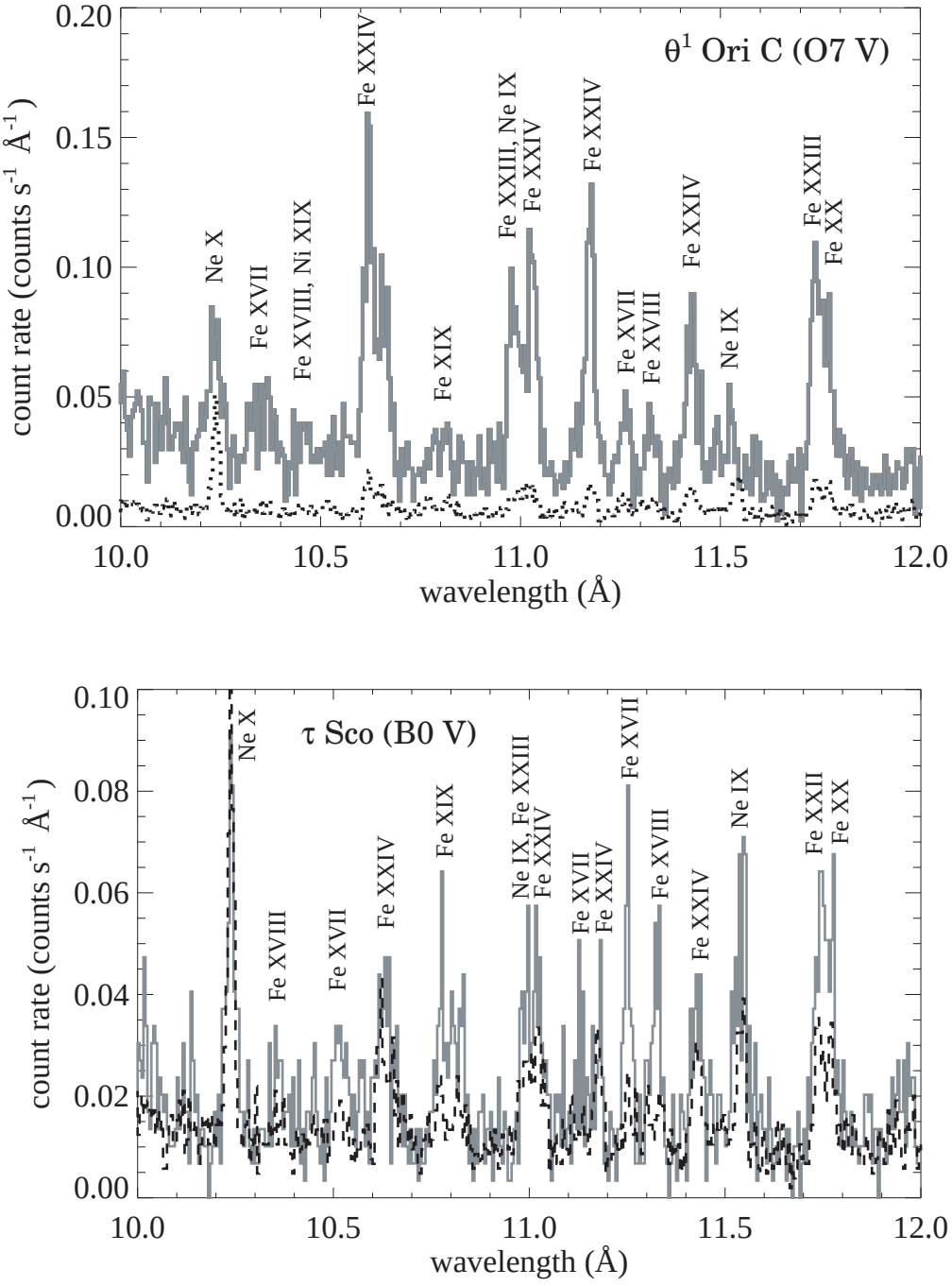

Figure 4. Upper panel: the MEG 10–12 Å spectrum of θ^1 Ori C shows strong, moderately broad, symmetric Fe XX–Fe XXIV lines indicating substantial emission measure at or above 16 MK. Lower panel: the τ Sco (B0 V) spectrum shows narrow Fe XX–Fe XXIV lines similar to those seen on the active corona of AB Dor (K1 V) (dashed lines).

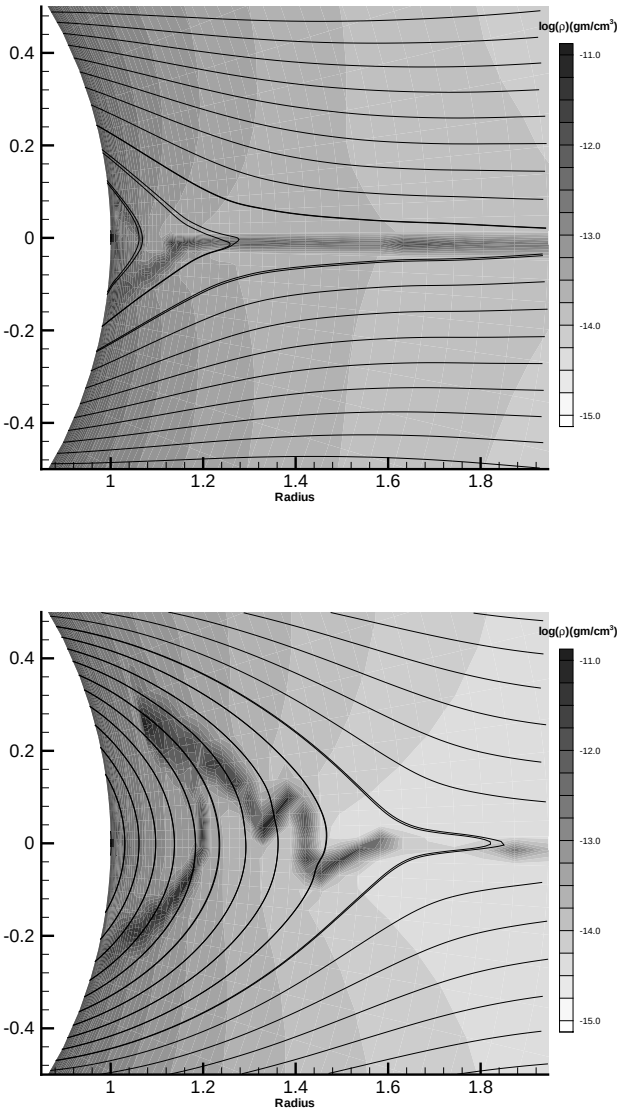

Figure 5. 2-D MHD simulations of an initially dipolar magnetic field distorted by radial mass loss on ζ Pup. Density (upper panels) and non-radial velocity contours (lower panels) at the end of two realizations: moderate magnetic confinement ($\eta = \sqrt{10}$, $t = 450$ ks) on the left and high confinement ($\eta = 10$, $t = 295$ ks) on the right. With sufficient confinement, material is accelerated to approximately ± 1000 km s^{-1} creating shocks in dense, unstable regions near the magnetic equator only $0.1 - 1 R_\star$ above the photosphere. The recent measurement of a 1.1-kG polar field on θ^1 Ori C implies $\eta \approx 13$ as on the right. The resulting dense, high-speed shocks may explain the broad, symmetric, high-temperature lines seen on θ^1 Ori C.

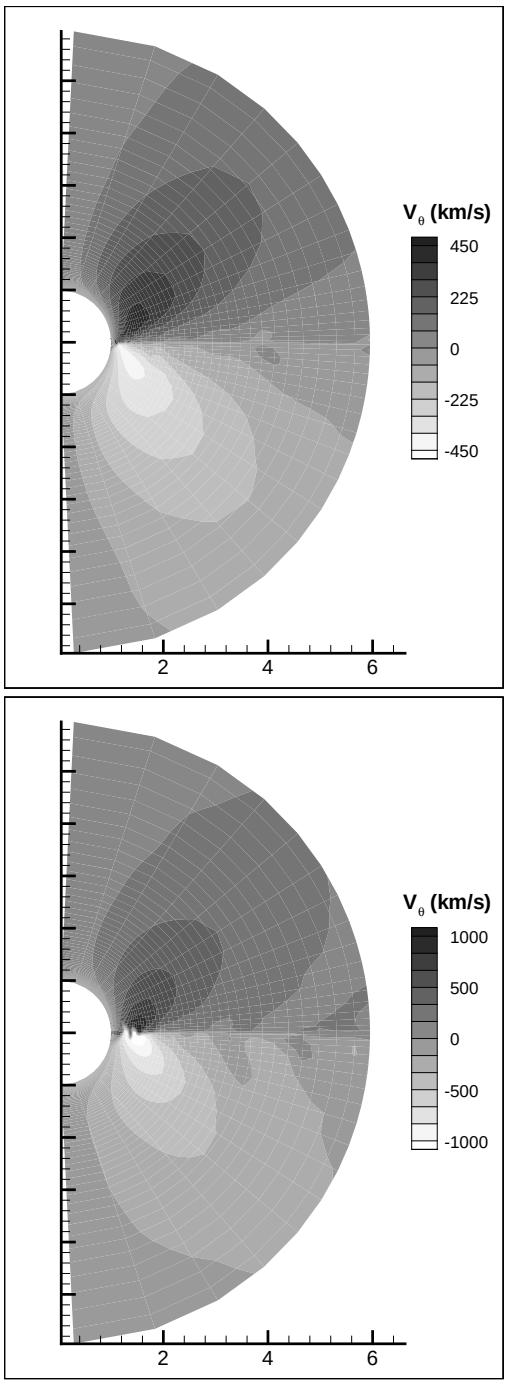
V$_\theta$ (km/s)
450
225
0
-225
-450
2
4
6
V$_\theta$ (km/s)
1000
500
0
-500
-1000
2
4
6

parameter,

$$\eta = \frac{B_0^2 R_\star^2}{\dot{M} v_\infty},$$

where B_0 is the surface equatorial field strength (approximately half the polar field strength). $\eta \gg 1$ implies the wind is confined by the field and $\eta \ll 1$ implies the field is completely stretched out by the wind.

In Figure 5, we show a pair of ζ Pup simulations for $\eta = \sqrt{10}$ and $\eta = 10$. For θ^1 Ori C, $B_0 \approx 550$ G and $\eta \approx 13$, implying high-speed shocks, $T \gtrsim 10^7$ K, and $n_{\rm e} \gtrsim 10^{10}$ cm^{-2}. As of this writing, we do not know if the wind continuum optical depth is low enough to view the entire volume of X-ray emitting plasma. Nonetheless, the 2-D simulations suggest that a moderately strong dipolar field can provide significant confinement and shock heating. To realistically test the MCWS idea, synthetic X-ray spectra based on 3-D MHD simulations of an oblique magnetic rotator are needed for a range of mass-loss rates, magnetic field geometries, and viewing angles.

6. Discussion

The velocity profiles, f/i ratios, and high plasma temperatures derived from *Chandra* spectra of OB stars suggest that magnetic fields may play an important role in the production of X-rays on young, massive stars. Time-resolved, high-resolution X-ray spectra of very young stars may help uncover the geometry of the underlying field. It is interesting to note that S1 Oph, θ^1 Ori C, and τ Sco, which show the most striking signs of magnetic activity, are all young and associated with star-forming regions: ρ Oph ($\lesssim 1$ Myr, André et al. 1988), Orion Nebula ($\lesssim 1$ Myr, Hillenbrand 1997), and Sco-Cen ($\lesssim 10$ Myr, Kilian 1994). Although a different kind of magnetic activity produces very hot, energetic X-ray flares seen on various classes of low-mass YSOs, both high-mass and low-mass stars undergo a brief episode of rapid accretion and mass-loss regulated by large-scale fields and disks. The evolution of the field and disk affects angular momentum evolution, planet formation, and the high-energy radiation environment of young planetary atmospheres.

References

André, P., Montmerle, T., Feigelson, E.D., Stine, P.C., & Klein, K. 1988, ApJ, 335, 940

Babel, J. , & Montmerle, T. 1997, A&A, 323, 121

Babel, J. , & Montmerle, T. 1997, ApJ, 485, L29

Cann, N.M. & Thakkar, A.J. 1992, Phys. Rev. A, 46, 9, 5397

Cassinelli, J.P., et al. 2001, ApJ, 554, L55

Corcoran, M., et al. 1994, ApJ, 436, L95

Cohen, D.H., Cassinelli, J.P., & MacFarlane, J.J. 1997, ApJ, 487, 867

Cohen, D.H., Cassinelli, J.P., & Waldron, W. 1997, ApJ, 488, 397

Cohen, D.H., Cooper, R.G., Macfarlane, J.J., Owocki, S.P., Cassinelli, J.P., & Wang, P. 1996, ApJ, 460, 506

Damiani, F. & Micela, G. 1995, ApJ, 446, 341

Drake, G.W.F. 1971, Phys. Rev. A, 3, 908

Feldmeier, A., Puls, J., Reile, C., Pauldrach, A., Kudritzki, R.P., & Owocki, S.P. 1995, Ap&SS, 233, 293

Gagné, M., Caillault, J.-P., Stauffer, J.R., & Linsky, J.L. 1997, ApJ, 478, L87

Gahm, G. F. 1980, ApJ, 242, L163

Ghosh, P., & Lamb, F.K. 1979, ApJ, 234, 296

Günther, E.W., Lehmann, H., Emerson, J.P., Staude, J. 1999, A&A, 341, 768

Harnden, F.R., Jr., et al. 1979, ApJ, 234, L51

Hillenbrand, L.A. 1997, AJ, 113, 1733

Hillier, D.J., et al. 1993, A&A, 276, 117

Johns-Krull, C.M., Valenti, J.A., & Koresko, C. 1999, ApJ, 516, 900

Kahn, S. et al. 2001, 365, L312

Kilian, J. 1994, A&A, 282, 867

Königl, A. 1991, ApJ, 370, L39

Lucy, L.B. & White, R.L. 1980, ApJ, 241, 300

MacFarlane, J.J. & Cassinelli, J.P. 1989, ApJ, 347, 1090

Owocki, S.P., Castor, J.I., & Rybicki, G.B. 1988, ApJ, 335, 914

Owocki, S.P., & Cohen, D.H. 1999, ApJ, 520, 833

Owocki, S.P., & Cohen, D.H. 2001, ApJ, in press, astro-ph/0101294

Pallavicini, R., et al. 1981, ApJ, 248, 279

Rebull, L.M., Wolff, S.C., Strom, S.E. , Makidon R. B. 2001, ApJ, in press, astro-ph/0105542

Reiners, A., Stahl, O., Wolf, B., Kaufer, A., Rivinius, T. 2000, A&A, 363, 585

Schulz, N., Canizares, C., Huenemoerder, D., & Lee, J.C. 2000, ApJ, 545, L135

Stahl, O., et al. 1993, A&A, 274, L29

Stahl, O., et al. 1996, A&A, 312, 539

Tsuboi, Y., Koyama, K., Hamaguchi, K., Tatematsu, K., Sekimoto, Y., Bally, J., & Reipurth, B. 2001, ApJ, 554, 734

Tsuboi, Y., Koyama, K., Murakami, H., Hayashi, M., Skinner, S., & Ueno, S. 1998, ApJ, 503, 894

Tsuboi, Y., Imanishi, K., Koyama, K., Grosso, N., & Montmerle, T. 2000, ApJ, 532, 1089

Walborn, N., & Nichols, J.S. 1994, ApJ, 425, L29

Waldron, W.L., & Cassinelli, J.P. 2001, ApJ, 548, L45

Yamauchi, S., Koyama, K., Sakano, M., & Okada, K. 1996, PASJ, 48, 719